Simultaneous measurements with 3D PIV and Acoustic Doppler Velocity Profiler

K. Blanckaert[1] and S. J. McLelland[2]

[1] ICARE-ENAC, Ecole Polytechnique Fédérale, CH-1015 Lausanne, Switzerland and Faculty of Civil Engineering and Geosciences, Delft University of Technology, Delft, The Netherlands, PH: +41 (0)21 6932378, koen.blanckaert@epfl.ch.

[2] Department of Geography, University of Hull, Cottingham Road, Hull, HU6 7RX, UK, PH +44 (0)1482 465007, s.j.mclelland@hull.ac.uk

ABSTRACT

Simultaneous velocity measurements were taken using Particle Image Velocimetry (PIV) and an Acoustic Doppler Velocity Profiler (ADVP) in a sharp open-channel bend with an immobile gravel bed. The PIV measures 3D velocity vectors in a vertical plane (~40cm x 20cm) at a frequency of 7.5 Hz, whereas the ADVP measures 3D velocity vectors in a vertical profile with a frequency of 31.25 Hz. The paper reports simultaneous measurements with both instruments positioned in the same location. Both instruments resolve accurately spatial structures of the complex mean flow fields characterized by small velocities of the order of 0.01 ms^{-1}, such as the outer-bank secondary flow cell and the secondary flow cell in the zone of flow separation at the inner bank. PIV measurements of the mean velocities are of better quality near the flow boundaries and the spatial distribution of data allows investigation of the temporal behaviour of secondary flow structures. Power spectra and time-series of quasi-instantaneous velocities demonstrate that the ADVP measures turbulence accurately, whilst PIV measurements of turbulence suffer from the lower temporal resolution and the higher noise levels. The results presented in this paper demonstrate that the combined application of PIV and ADVP allows investigation complex 3D flows in greater detail than is possible from a single instrument.

INTRODUCTION

This paper combines the use of three-dimensional Particle Image Velocimetry (PIV) with an Acoustic Doppler Velocity Profiler (ADVP) to examine the spatial structure of a complex flow field. The flow examined is at a cross-section in a sharp meander bend with flow separation at the inner bend over an immobile rough gravel bed. Both instruments were deployed simultaneously at the same cross-section in the flow. ADVP measurements were obtained from ten vertical profiles whilst the PIV was used to traverse the same cross-section with eight overlapping flow maps to cover the entire cross-section.

The aim of this paper is to compare the performance of the two different instruments and to assess the advantages and disadvantages of each technique. Comparison will be made between the spatial resolution and coverage of the two instruments, the mean flow structure, and key measures of flow turbulence.

PIV has the advantage that three-dimensional velocities can be obtained from a large measurement plane simultaneously. In this case each measurement plane covered almost half the channel width. However, in comparison to the ADVP the temporal resolution of the PIV measurements is significantly lower and measurement accuracy depends on many complex factors such as flow seeding. These factors combined have important consequences for measuring the turbulent flow parameters.

EXPERIMENTAL SET-UP AND CONDITIONS

The experiments were undertaken in the Total Environment Simulator flume at Hull University. The working section of the flume is 6m wide and 11m long. Within this area a flow channel with two sharp bends was constructed as shown in Figure 1. The walls of the curved central section of the flow channel were constructed from clear Perspex to enable imaging through the channel sidewalls. The areas of the flume outside the flow channel were also flooded with water to enable the PIV system to view into the channel without any refractive effects. The channel bed was filled with coarse bed material with a D_{50} of 11.8mm and an average downstream slope of 0.002.

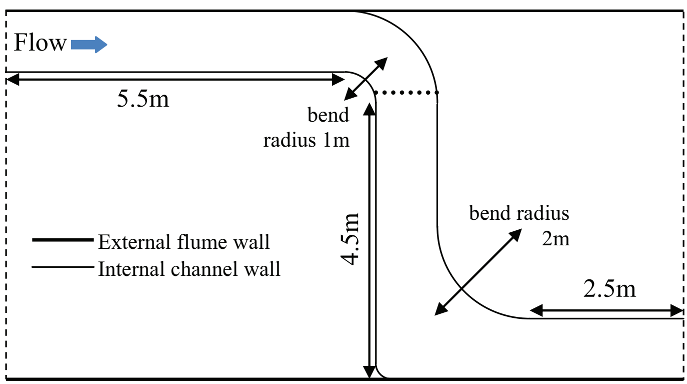

Figure 1. Schematic drawing of the flume set-up. The flow channel was 1m wide and the dotted line shows the location of the measurement section.

The investigated flow was rough turbulent and characterized by flow depth of ~0.14m, an overall velocity of ~0.55ms^{-1} and a Froude number of ~0.5. Flow measurements were taken just downstream apex of the first bend at a cross-section parallel to the inlet flow direction. This cross-section is not perpendicular to the channel centreline: the outer-bank, centreline and inner bank in the cross-section are situated at 81.6°, 77.34° and 64.4° in the bend, respectively. Figure 2 shows the ADVP mounted near the centre of the channel and the PIV system positioned outside the Perspex channel wall.

Figure 2. Photograph showing ADVP located near the centre of the channel and PIV system outside the channel (the light sheet optics are in the centre of the black tube and the cameras are inside the tube with mirrors at either end to view the flow field).

3D Particle Image Velocimetry (PIV). Three-dimensional Particle Image Velocimetry (PIV) was obtained using a Dantec system that comprises, a New Wave Research Solo double-pulsed Nd:YAG laser (pulse duration 10 ns, time delay between pulses 2 ms), two Kodak Megaplus ES1.0 digital cameras (8-bit, 1016 x 1008 pixels and a Dantec System Hub to synchronize the image acquisition with the laser pulsing and to store the acquired image data. A submersible optic system was fitted to the laser to expand the beam and deliver a ~5 mm thick sheet of light below the water surface aligned normal to the bed surface and parallel to the inlet flow channel. The two cameras were submersed below the water surface with remote focus, scheimpflug and aperture control and imaged the light sheet through the Perspex channel walls.

The two cameras imaged a stereoscopic measurement area of 483 mm across the channel and 262 mm in the vertical plane. PIV measurements were made at 100mm intervals across the channel ensuring substantial overlap between images. The flow depth was ~140 mm therefore the images were cropped to remove data below the bed surface and above the water surface. Measurements were taken for 4 minutes at each location at a measurement frequency of 7.5 Hz. The images from each location were processed using Dantec FlowManager software into vector maps using an interrogation area of 64 x 32 pixels and an overlap of 25%. For each image this yields 17 x 21 vectors within the area of interest. The time-averaged vector maps and turbulence statistics from each measurement location were then combined by kriging to produce a map of the flow across the entire cross-section.

Acoustic Doppler Velocity Profiler (ADVP). Non-intrusive velocity measurements were made with an ADVP developed at EPFL (Lemmin and Rolland 1997, Hurther and Lemmin 1998). It consists of a central emitter surrounded by four receivers (Figure 2), placed in a water-filled housing that touches the water surface. In this configuration, the ADVP measures vertical profiles of the three-dimensional velocity vector, which are divided into identical bins with a height of 3.75 mm. Three receivers would be sufficient to measure the three-dimensional velocity vector, but the addition of a fourth receiver improves turbulence measurements (Hurther and Lemmin 2001, Blanckaert and Lemmin 2006). The flow was seeded with hydrogen bubbles generated by means of electrolysis (Blanckaert and Lemmin 2006) in order to guarantee a sufficient acoustic scattering level. An ADVP configuration was adopted with the four receivers symmetrically surrounding the emitter and at angle of 45° with respect to the measured cross-sections. Due to the physical dimensions of this ADVP configuration it was not possible to measure closer than 0.18 m to the inner and outer banks. This is not an inherent limitation of the ADVP, however, and an asymmetrical ADVP configuration with all four receivers placed at the same side of the emitter has already been applied to measure within 0.02 m from vertical banks (Blanckaert 2002). Measurements were taken in 10 vertical profiles for at least 6 minutes at each location at a measuring frequency of 31.25 Hz. Patterns of flow quantities across the entire measuring grid are obtained by interpolation in-between measured profiles. Blanckaert and de Vriend (2004) estimate the uncertainty in the experimental data at 4% in the magnitude of the time-averaged velocity, 10% in time-averaged secondary flow components, 15% in the turbulent shear stresses, 20% in the turbulent normal stresses and the turbulent kinetic energy. The accuracy in the ADVP measurements is reduced near the flow boundaries. At the water surface, the ADVP housing perturbs the flow up to 15 mm below the water surface. In a region up to 15 mm from solid boundaries, the ADVP appears to underestimate turbulent characteristics, which is tentatively attributed to the high velocity gradients within the measuring volume and/or to parasitical echoes from the solid boundary (Hurther and Lemmin 2001).

RESULTS

Time-averaged flow patterns. Figure 3 shows the time-averaged magnitude of the velocity vector measured using the ADVP and PIV. In general the data show a good correlation between the measured velocities in the core of the flow domain, however, the magnitude of the velocities measured by the PIV are slightly lower than those measured by the ADVP. The flow perturbation induced by the ADVP housing at the water surface is visible in the PIV and ADVP measurements. The PIV measurements provide better data near the bed, where the ADVP measurements are perturbed. Moreover they allow measuring the near-bank regions, which are still poorly understood in spite of their importance with respect to bank protection, bank erosion/accretion and river planform evolution.

The velocity pattern suggests the existence of complex three-dimensional flow patterns. The core of high velocities shown by both instruments at $y \approx 0.2$m - 0.4m and $z/H \approx 0.5$-0.8 and the inclination of the velocity isolines in the central part of the cross-section indicate the existence of a curvature-induced central secondary flow cell. This cell advects high near-surface velocities outwards in the upper part of the water column, and low near-bed velocities inwards in the lower part of the water column. The bulging of the isolines near the outer-bank measured with the PIV suggests the existence of a counter-rotating outer-bank secondary flow cell. This cell advects low velocities originating from the outer-bank boundary layer towards the core of the flow domain near the water surface, and high velocities originating from near the water surface towards the outer bank. PIV measurements also show a zone of low velocities near the inner bank that widens towards the water surface. Pronounced velocity gradients occur along a layer that is steeply inclined from about $y \approx 0.2$ m near the surface to the bed at the inner bank. These features are characteristic of flow separation at the inner bank.

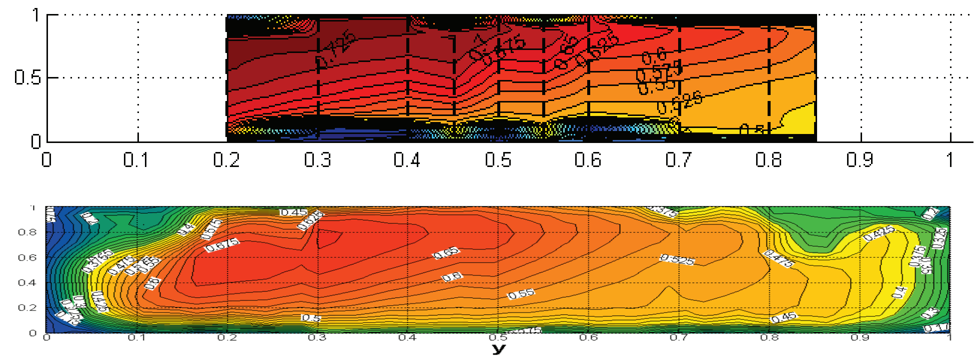

Figure 3. Pattern of the magnitude of the velocity vector. Distance from the inner bank on the horizontal axis and normalized flow depth on the vertical axis. Undistorted scale. (top) interpolated from ADVP measurements in vertical profiles indicated by dashed lines; (bottom) 3D PIV measurements.

Flow separation at the inner bank, the outer-bank secondary flow cell and the centre-region secondary flow cell leave a clear footprint on the velocity pattern. These observations indicate the important role of secondary flow structures with respect to the (re)distribution of momentum and boundary shear stress in complex three-dimensional flows. In laboratory investigations, secondary flow is usually defined as the flow component in cross-sections perpendicular to the channel centreline. However, the orientation of the measured cross-section is not perpendicular to the centreline which complicates the visualisation of the secondary flow pattern. A clear indication of the secondary flow pattern is given by the vertical velocities as shown in Figure 4. The patterns measured with the ADVP and PIV are qualitatively in very good agreement, although some quantitative differences exist that can largely be attributed to slight differences in vertical alignment of both instruments. Both instruments are able to measure and visualize secondary flow structures characterized by small velocities of the order of 0.01 ms^{-1}.

These vertical velocity patterns confirm the findings based on the magnitude of the velocity vector and clearly show three secondary flow cells. The typical curvature-induced centre-region cell is situated in the zone y = 0.20m – 0.85m and has maximum vertical velocities of about 0.03ms^{-1}. The maximum downwelling velocities are found about one flow depth away from the outer bank, which indicates the existence of an outer-bank cell. A secondary flow cell that co-rotates with the centre-region cell is discernable in the flow separation zone near the inner bank.

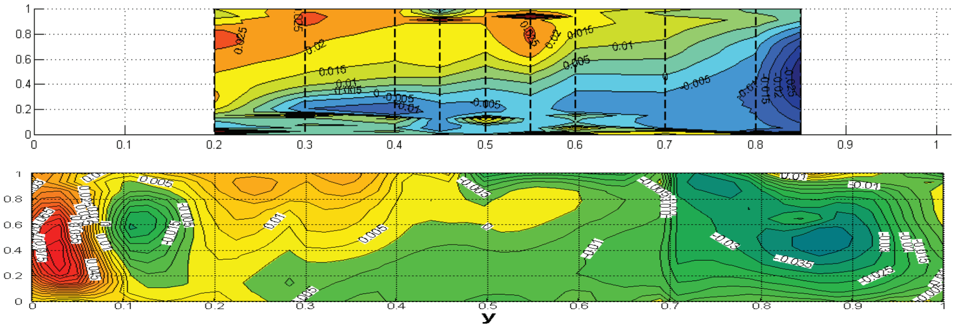

Figure 4. Pattern of the vertical velocity. (top) ADVP measurements in vertical profiles indicated by dashed lines; (bottom) 3D PIV measurements.

Turbulence. Figure 5 shows the measurement of turbulent kinetic energy (TKE). The spatial distribution and magnitude of TKE measured with the PIV and ADVP show a number of differences that highlight the different capabilities of the instruments as well as the complex nature of the flow being investigated. PIV and ADVP measurements show similar trends in the central zone, although PIV measurements are consistently higher. Measurements from the PIV show very high TKE within the flow separation zone identified from mean flow measurements above whereas ADVP measurements show the opposite trend. It is likely that PIV measurements in this area are significantly affected by noise due to the seeding density which is difficult to control in the flow separation zone. ADVP measurements have proven to be reliable under similar flow conditions (Zeng et al. 2008). The power spectra and cumulative power spectra (Figure 6) at mid-depth from $y = 0.3$ m confirm the good quality of the ADVP measurements: they show an inertial sub-range characterized by a -5/3 slope for frequencies higher than about 5Hz and a tendency towards isotropy for frequencies higher than about 10 Hz.

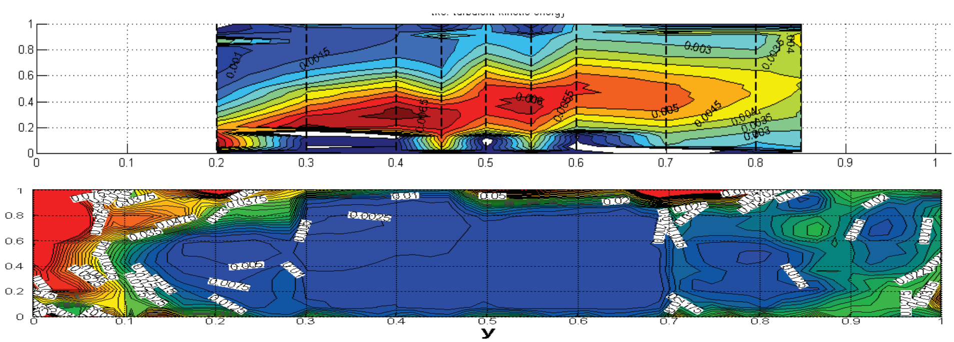

Figure 5. Pattern of the turbulent kinetic energy. (top) ADVP measurements in vertical profiles indicated by dashed lines; (bottom) 3D PIV measurements.

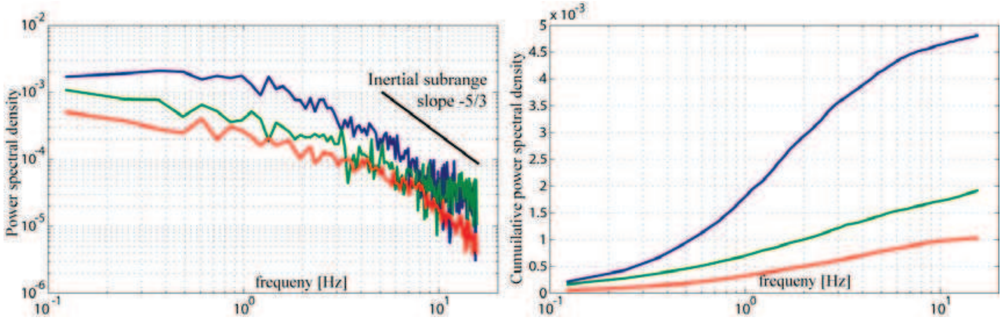

Figure 6. Power spectra (left) and cumulative power spectra (right) of the velocity fluctuations along *x* ,*y* ,*z* measured in the point at *y* = 0.3m at mid-depth.

The temporal resolution of the PIV measurements does not allow detailed investigation of turbulent coherent structures, but it is expected to be sufficient for the investigation of the temporal behaviour of secondary flow cells, which is characterized by lower frequencies of the order of 1Hz (Blanckaert and de Vriend 2005).

A 5 second time-series of the quasi-instantaneous streamwise-vertical velocity components in the vertical plane at 0.3m from the inner bank, shown in Figure 7, illustrates that the spatial (vertical axis) and temporal (horizontal axis) resolution of the ADVP measurements is considerably higher than that of the PIV measurements. Hurther et al. (2007) have demonstrated that the temporal and spatial resolutions of the ADVP measurements allow detailed investigation of turbulent coherent structures.

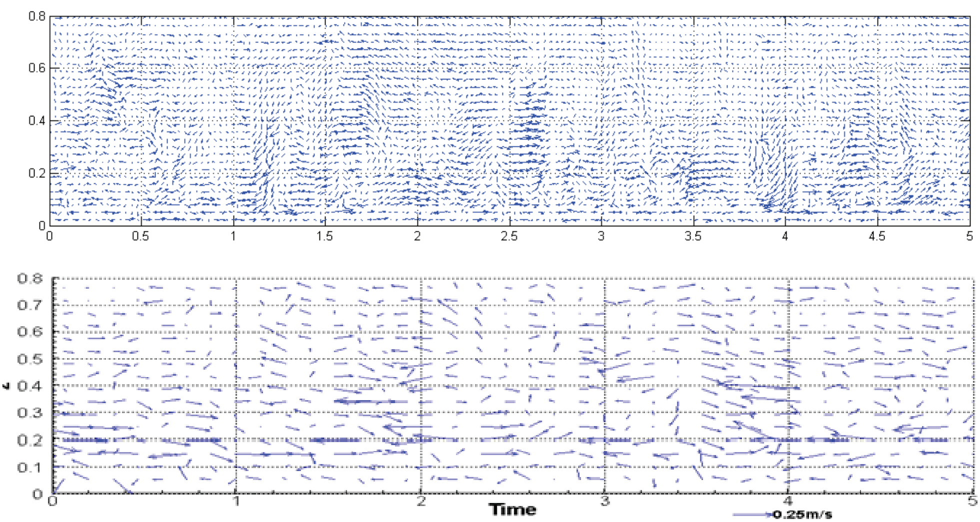

Figure 7. Pattern of instantaneous streamwise-vertical velocity components in the vertical plane at 0.3m from the inner bank based on the Taylor hypothesis of frozen turbulence. (top) ADVP measurements; (bottom) 3D PIV measurements. Illustrated time series were not measured simultaneously.

CONCLUSIONS AND DISCUSSION

The results presented in this paper demonstrate that the combined application of PIV and ADVP produces greater detail than is possible from a single instrument. Both instruments are able to measure spatial structures of complex 3D mean flow fields characterized by small velocities of the order of 0.01 ms^{-1}. PIV measurements are of better quality near the flow boundaries, whilst ADVP appears to be considerably better for turbulence measurements where PIV suffers from lower temporal resolution and higher noise levels.

The simultaneous application of PIV and ADVP in complex three-dimensional flows allows exploiting the strengths and circumventing weaknesses of both instruments. The temporal resolution of PIV measurements allows investigating the time-averaged flow patterns as well as the temporal behaviour of secondary flow cells (not shown in the paper). Simultaneous ADVP measurements allow investigating in more detail turbulence characteristics as well as coherent turbulent structures.

ACKNOWLEDGEMENTS

The reported laboratory experiments were supported by the European Community's Sixth Framework Programme through the grant to the budget of the Integrated Infrastructure Initiative HYDRALAB III, Contract no. 022441 (RII3). The authors would also like to thank M.G. Kleinhans, A. van de Kruijs, B.J. Murphy, O. Owodunni, D.R. Parsons, W.S.J. Uijttewaal, and R.J. Hardy.

REFERENCES

Blanckaert, K. (2002). “Flow and turbulence in sharp open-channel bends.” Ph.D. thesis No. 2545, Ecole Polytechnique Fédérale Lausanne, Switzerland, "ftp://lrhmac15.epfl.ch/Pub/Thesis/Blanckaert/PhD".

Blanckaert, K., and de Vriend, H. J. (2004). “Secondary flow in sharp open-channel bends.” *J. Fluid Mech.,* 498, 353–380.

Blanckaert, K. & de Vriend, H. J. (2005). “Turbulence structure in sharp open-channel bends.” *J. Fluid Mech.*, 536, 27-48.

Blanckaert, K., and Lemmin, U. (2006). “Means of noise reduction in acoustic turbulence measurements.” *J. Hydraul. Res.*, 44(1), 3–17.

Hurther, D., and Lemmin, U. (1998). ‘‘A constant beamwidth transducer for three-dimensional Doppler profile measurements in open channel flow.’’ *Measurement Science and Technology*, 9(10), 1706–1714.

Hurther, D., and Lemmin, U. (2001). ‘‘A correction method for turbulence measurements with a 3-D acoustic Doppler velocity profiler.’’ *J. Atm. Oc. Techn*, Vol. 18, 446–458.

Hurther, D., Lemmin, U. and Terray, E.A. (2007). “Turbulent transport in the outer region of rough-wall open-channel flows: the contribution of large coherent shear stress structures (LC3S)”. *J. Fluid Mech.*, 574, 465-493.

Lemmin, U., and Rolland, T. (1997). ‘‘Acoustic velocity profiler for laboratory and field studies.’’ *J. Hydr. Engrg.*, ASCE, 123(12), 1089–1098.

Zeng J., Constantinescu G., Blanckaert K. and Weber L. (2008). "Flow and bathymetry in sharp open-channel bends: experiments and predictions." *Water Resour. Res.*, 44, W09401, doi:10.1029/2007WR006303.